Applied Energy xxx (2015) xxx–xxx

Contents lists available at ScienceDirect

Applied Energy

journal homepage: www.elsevier.com/locate/apenergy

High-stability, high-capacity oxygen carriers: Iron oxide-perovskite composite materials for hydrogen production by chemical looping

Cristina Dueso, Claire Thompson, Ian Metcalfe *

Newcastle University, Merz Court, NE1 7RU Newcastle upon Tyne, United Kingdom

HIGHLIGHTS

- Composite materials (Fe_2O_3 clusters within a LSF731 matrix) were prepared.
- Two preparation methods were used: mechanical mixing and a modified Pechini method.
- Composite reactivity was not the addition of Fe_2O_3 and LSF731 reactivity.
- Composite materials showed better stability than iron oxide with cycling.
- Hydrogen production was considerably higher than with either Fe_2O_3 or LSF731 alone.

ARTICLE INFO

Article history:
Received 12 December 2014
Received in revised form 30 April 2015
Accepted 19 May 2015
Available online xxxx

Keywords:
Hydrogen production
Chemical looping
Perovskite
Iron oxide
Composite
Oxygen carrier material

ABSTRACT

Iron oxide has been widely used as an oxygen carrier material (OCM) for hydrogen production by chemical looping due to its favourable thermodynamic properties. In spite of this, iron oxide loses much of its activity after redox cycling mainly due to sintering and agglomeration. Perovskites, such as $La_{0.7}Sr_{0.3}FeO_{3-\delta}$ (LSF731), have been suggested as potential candidate OCMs for hydrogen production due to their excellent oxygen transport properties and stability under cycling. However, hydrogen production per cycle for a similar carrier weight is lower than with iron oxide. This work proposes the use of composite OCMs made of iron oxide clusters embedded in an LSF731 matrix. The perovskite matrix facilitates oxygen transport to the iron oxide clusters while preventing agglomeration. Two preparation methods, mechanical mixing and a modified Pechini method, were used to obtain composite materials with different iron oxide weight fractions, 11 and 30 wt.%. The reactivity of these OCMs was studied in a thermogravimetric analyser. Hydrogen production and carrier stability were investigated in a microreactor over 25 redox cycles while periodically feeding carbon monoxide and water in order to produce carbon dioxide and hydrogen in separate streams. Hydrogen production was stable over 25 cycles for LSF731 and the composite OCM with 30 wt.% iron oxide produced by the modified Pechini method but iron oxide particles alone underwent a decrease in the hydrogen production with cycling. The hydrogen production during the 25th cycle was eight times higher for the composite material than for iron oxide alone and four times higher than for LSF731. The hydrogen production was therefore also higher than that expected from a simple combination of the iron oxide and LSF731 alone, indicating a synergetic effect whereby the LSF731 may have a higher effective oxygen capacity when in the form of the composite material.

1. Introduction

Chemical looping hydrogen production typically utilises iron oxide as an oxygen carrier as this material has several thermodynamically favourable phase changes that can be exploited [1–4]. In this process a carbonaceous fuel, here carbon monoxide, is used to reduce the iron oxide (producing carbon dioxide). Then water is used to re-oxidise the iron and produce hydrogen. This is performed in a cyclic manner. In order to have good utilisation of the redox capacity of the material, we need to use an oxygen carrier material (OCM) particle size, *l*, that is similar to or less than the effective oxygen diffusional lengthscale (effective diffusion coefficient, *D*, divided by an equivalent first order surface rate constant, *k*) such that the surface rate is controlling, e.g. *l* is similar to or less than *D*/k. The diffusional lengthscale of oxygen within iron oxide is

* Corresponding author. Tel: +44 (0)191 222 5279.
E-mail address: i.metcalfe@ncl.ac.uk (I. Metcalfe).

http://dx.doi.org/10.1016/j.apenergy.2015.05.062
0306-2619/

expected to be quite short as loss of surface area in iron oxide OCMs significantly affects effective OCM capacity [5,6]. Therefore a small particle size is required, which in turn means that a large surface area is required. Iron oxide, however, suffers from thermal sintering at high temperatures (>800 °C) and as a result loses surface area while particle size increases.

These problems could be overcome if the iron oxide was embedded and well dispersed in a stable matrix. This matrix should have a diffusional lengthscale for oxygen comparable to or larger than its particle size. Doped lanthanum ferrites are known to have a relatively long effective diffusional lengthscale for oxygen with, e.g., $La_{0.9}Sr_{0.1}FeO_{3-\delta}$ (LSF911) having a diffusional lengthscale of around 60 μm at 900 °C [7]. Here we use $La_{0.7}Sr_{0.3}FeO_{3-\delta}$ (LSF731) as the matrix with particle sizes of 80–160 μm albeit at the slightly lower temperature of 850 °C in the isothermal work. Thus we may expect, if the properties of LSF911 and LSF731 are not dissimilar and the temperature difference has limited impact, that the diffusional lengthscale of LSF731 is similar to its particle size. This matrix material does not in itself require a high oxygen capacity on redox cycling (this capacity being provided by the iron oxide), rather it provides a rapid oxygen transfer pathway to access a distributed reserve of iron oxide and prevents excessive sintering of iron oxide. It is expected that the composite material would effectively combine the benefits of both materials individually, i.e. the high oxygen capacity of the iron oxide and the superior stability and oxygen transport properties of LSF731 [8].

The idea of embedding the oxygen carrier within a stable matrix was first suggested by Thursfield et al. [1]. Galinsky et al. [9] prepared an OCM containing 60 wt.% iron oxide supported on $La_{0.8}Sr_{0.2}FeO_3$ by solid-state synthesis (SSR). Reactivity tests performed in a TGA showed that the presence of LSF enhanced the reactivity of the OCM with H_2, CO and CH_4 5-70-fold compared with inert supports, such as TiO_2, and reduced carbon formation. The authors proposed that the use of a mixed ionic-electronic conductive (MIEC) support facilitated O^{2-} transport from the iron oxide and improved the resistance of the material. The same research group investigated the influence of the preparation method on the performance of Fe_2O_3@$La_xSr_{1-x}FeO_3$ OCMs for partial oxidation of methane [10]. A sol–gel method obtained an OCM which was more reactive and exhibited less carbon formation than the one prepared by SSR. An OCM combining iron oxide and $CaTi_{0.85}Fe_{0.15}O_{3-\delta}$ (CTF) showed better properties for syngas conversion than composite materials with other perovskites, such as LSF and BCF ($BaCe_{0.7}Fe_{0.3}O_{3-\delta}$), due to a higher stability [11] and indeed redox properties in general appear to be affected by support-iron oxide interactions [12]. Iron oxide supported on $Ca_{0.8}Sr_{0.2}Ti_{0.8}Ni_{0.2}O_3$ presented better stability and less carbon formation with CH_4 as fuel than when CeO_2 and $MgAl_2O_4$ were used as supports. Substitution of Ni^{2+} on the B-site with Fe^{3+} improved the perovskite structure stability.

This work aims to definitively prove the idea that well-dispersed clusters of iron oxide embedded in an LSF731 matrix can improve the stability and maintain the reactivity of the OCM on repeated cycling.

2. Experimental

2.1. OCM preparation

Several materials with a composite structure made of iron oxide clusters embedded in a matrix of LSF731 were prepared in this work to be used as OCMs for hydrogen production by chemical looping. Fig. 1 shows a schematic diagram of the OCM particles. Iron oxide is defined to be in the form of a cluster when located within the LSF731 matrix. Otherwise the iron oxide may be in the form of a particle (>40 μm) or powder (<40 μm). Two different preparation methods, mechanical mixing and a modified Pechini method, are described below.

2.1.1. Mechanical mixing

To prepare the composite materials by the mechanical mixing method, commercial sub-micron powders of LSF731 and iron oxide were mixed in two different mass ratios: 7:3 and 8.9:1.1. Pellets of 2 g were formed from these mixtures by applying 1500 kgf/cm^2 for 30 s with a hydraulic press, followed by sintering at 1250 °C in air for 4 h in a tubular furnace. The desired particle size was obtained by crushing and sieving the pellets (80–160 μm). This resulted in iron oxide clusters embedded in an LSF731 matrix.

The effect of the iron oxide cluster size was also studied. For this purpose, OCM particles were prepared by mixing commercial LSF731 sub-micron powder and iron oxide powder with a size range of 20–40 μm following the method described above. These 20–40 μm powders were obtained from pellet formation from the iron oxide sub-micron powders, calcination at 1250 °C for 4 h, crushing and sieving to 20–40 μm.

OCM particles containing only either iron oxide or LSF731 were also prepared as reference materials. Particles in the range 80–160 μm were made from commercially available iron oxide sub-micron powders. 2 g of the powders were pelletized with the hydraulic press, sintered at 1250 °C in air for 4 h in the tubular furnace, crushed and sieved to 40–80 μm and 80–160 μm particle sizes. The same process was also employed to fabricate LSF731 particles of specific particle sizes (80–160 μm).

2.1.2. Pechini method

OCMs with a composite structure containing LSF731 and iron oxide were prepared from the metallic nitrates using a modified Pechini method. Reaction (1) shows the stoichiometry for the LSF731 preparation which was chosen such that the amount of ammonium nitrate was minimized and the by-products were gaseous water, carbon dioxide and nitrogen.

$$0.7[La(NO_3)_3 \cdot 6H_2O] + 0.3\ Sr(NO_3)_2 + Fe(NO_3)_3 \cdot 9H_2O + 1.684C_6H_8O_7 + 0.858NH_4NO_3 \rightarrow La_{0.7}Sr_{0.3}FeO_3 + 10.105\ CO_2 + 21.653H_2O + 3.708\ N_2 \quad (1)$$

Stoichiometric amounts of the metal nitrates, $La(NO_3)_3{\cdot}6H_2O$, $Sr(NO_3)_2$ and $Fe(NO_3)_3{\cdot}9H_2O$, citric acid and ammonium nitrate were dissolved in de-ionized water separately and stirred for 30 min to get clear solutions. Citric acid was used as a complexation agent while ammonium nitrate acted as an igniter, accelerating the combustion process. The ammonium nitrate solution was added after the citric acid to the nitrate solution. To ensure good mixing of all the constituents, the final solution was stirred for one hour.

Either iron oxide sub-micron powders or iron oxide 20–40 μm powders were added later to this mixture in the right proportion to get a mass ratio in the final material of 7:3 or 8.9:1.1. The solution was then transferred to a 2 L beaker and heated gradually on a hot plate up to ~200 °C inside a fume cupboard. As the water evaporation in the mixture neared completion, the solution turned brownish and viscous. Finally, in the form of a gel, it combusted with visible flames releasing gases according to reaction (1). The fluffy powder obtained was homogenised in a pestle and mortar and packed into ceramic crucibles to be dried overnight at 80–100 °C. After that, the solid was calcined in air at 800 °C for 2 h to convert the amorphous gel into crystalline LSF731. To obtain a suitable particle size for the chemical looping reactors, pellets were prepared from the obtained powders by uniaxially pressing approximately 2 g of the material and sintering at 1200 °C in air

Please cite this article in press as: Dueso C et al. High-stability, high-capacity oxygen carriers: Iron oxide-perovskite composite materials for hydrogen production by chemical looping. Appl Energy (2015), http://dx.doi.org/10.1016/j.apenergy.2015.05.062

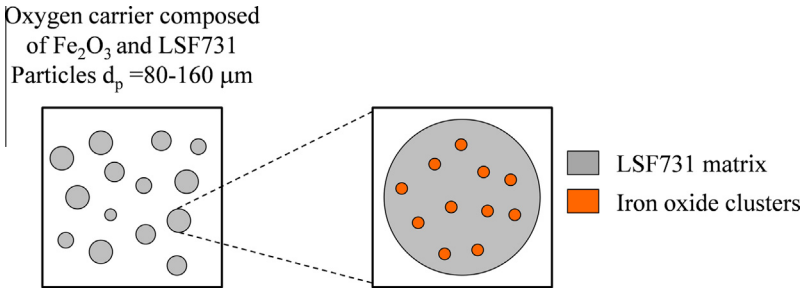

Fig. 1. Schematic diagram of the OCM composite particles.

for 6 h. These pellets were subsequently crushed and sieved (80–160 μm).

Table 1 shows all the OCMs prepared for this work by different methods. The composite materials are designated with LSF followed by the weight fraction content of iron oxide and the first letters of the preparation method, MM for mechanical mixing and Pec for the modified Pechini method. The letter P indicates that sub-micron iron oxide powders were used while 20–40 indicates that 20–40 μm iron oxide powders were utilized in the preparation of the OCMs.

2.2. Thermogravimetric analysis

The reactivity of the materials for hydrogen production from water splitting by chemical looping was studied in a thermogravimetric analyser Mettler-Toledo TGA/DSC 1 at atmospheric pressure and 850 °C. The particles were exposed alternatively to reducing and oxidising conditions. Three redox cycles were performed in all cases. A permanent flow of nitrogen of 50 ml STP/min (all flowrates are measured at STP) was used as protective gas for the balance. In addition to this flow, the reacting gas (50 ml/min) was fed to the TGA reactor during the operation. Prior to reacting with the solid sample, the reactive gas was mixed with the protective gas. The initial sample mass used in the TGA experiments was always 20–21 mg.

During the reduction period, 10% of carbon monoxide in nitrogen was introduced in the TGA for 30 min. This time was selected as a compromise to perform as many tests as possible while the duration was sufficient to study the kinetics of the reaction. After this, nitrogen was fed for 15 min to avoid the mixing of the reducing and the oxidising gases. The oxidation took place in two different stages. First, the particles were oxidized by 10% carbon dioxide in nitrogen for 20 min. Following a 15 min nitrogen purge, samples were fully oxidized with air for 10 min in order to return to the initial state.

In chemical looping, hydrogen is produced from water splitting during the oxidation with water. Nevertheless, in these experiments water was substituted by carbon dioxide, thermodynamically equivalent at 850 °C. The values of ΔG for reactions (2) and (3) at 850 °C are very similar, as well as the corresponding equilibrium constants. The validity of the substitution of steam by carbon dioxide was experimentally verified in a previous work by Liu et al. [13] reproducing the same cyclic conversion in a fluidized bed at 850 °C with both gases.

$$3Fe + 4H_2O(g) \rightarrow Fe_3O_4 + 4H_2(g) \quad \Delta G_{850^\circ C} = -12.234\ \text{kJ/mol} \quad (2)$$

$$3Fe + 4CO_2(g) \rightarrow Fe_3O_4 + 4CO(g) \quad \Delta G_{850^\circ C} = -16.391\ \text{kJ/mol} \quad (3)$$

2.3. Cycling operation in a microreactor

In order to determine the amount of hydrogen produced and the stability of the materials with time, 25 redox cycles were performed in a fully automated and programmable gas supply microreactor (CATLAB, Hiden Analytical, UK) at 1 atm and 850 °C. After the fresh sample (~50 mg) was placed inside, the microreactor was flushed with a helium flow of 50 ml/min prior to commencing testing. Each sample was subjected to multi-cycle isothermal reduction under 5% carbon monoxide in helium and isothermal oxidation under 5% water in helium with inlet flow rates of 50 ml/min. Reduction and oxidation steps were performed for 30 min. Helium was flushed for 15 min after reduction and oxidation in order to evacuate the reactor of any reactive gas or any product and to avoid mixing of the reducing and oxidising gases. The outlet gases of the microreactor, i.e. carbon monoxide, carbon dioxide, hydrogen, water and helium, were fed into a soft ionisation quadrupole mass spectrometer (QMS) through a heated capillary line for continuous online analysis. Temperature of the sample was monitored and controlled by an internal K-type thermocouple inserted into an inert alumina sleeve. Water was delivered into the microreactor by a saturator system (Grant, UK) using helium as a

Table 1
Properties of the OCMs prepared in this work.

Sample	Preparation method	Iron oxide content (%)	Particle size (μm)	Cluster size (μm)	BET (m^2/g)
LSF731	MM	N/A	80–160	N/A	0.10
FeP	As received	100	Sub-micron	N/A	25.5
Fe40-80	MM	100	40–80	N/A	Unavailable
Fe80-160	MM	100	80–160	N/A	0.125
LSF-30Fe-Pec-P	Pechini	30	80–160	Sub-micron	4.97
LSF-30Fe-Pec-20-40	Pechini	30	80–160	20-40	1.10
LSF-11Fe-Pec-P	Pechini	11	80–160	Sub-micron	0.47
LSF-11Fe-Pec-20-40	Pechini	11	80–160	20–40	0.29
LSF-30Fe-MM-P	MM	30	80–160	Sub-micron	0.79
LSF-30Fe-MM-20-40	MM	30	80–160	20–40	<0.01
LSF-11Fe-MM-P	MM	11	80–160	Sub-micron	<0.01
LSF-11Fe-MM-20-40	MM	11	80–160	20–40	Unavailable

Please cite this article in press as: Dueso C et al. High-stability, high-capacity oxygen carriers: Iron oxide-perovskite composite materials for hydrogen production by chemical looping. Appl Energy (2015), http://dx.doi.org/10.1016/j.apenergy.2015.05.062

carrier. The set point of the water bath was 30.1 °C which corresponds to a water mole fraction of 4.2% in the carrier gas at atmospheric pressure. Nevertheless, the water fraction measured by a cold mirror dew point hygrometer (CMH-1, Alpha Moisture Systems, UK) used to calibrate the water signal for the QMS, indicated that this value oscillated between 5.0 and 5.5%, depending on the lab temperature. These differences are taken into account later.

2.4. Characterisation

Fresh OCM particles were physically and chemically characterised by several techniques. BET surface area was determined by adsorption/desorption of nitrogen at 77 K in a Beckman Coulter SA3100 instrument. The microstructure of the particles and elemental distribution in the solids were observed by a scanning electron microscope (SEM) XL30 ESEM-FEG equipped with a Rontec Quantax EDX analyser. The identification of crystalline chemical species was carried out by powder X-ray diffraction performed in a PANalytical X'Pert Pro Multipurpose Diffractometer (MPD).

3. Results and discussion

3.1. Characterisation

SEM analysis was used to determine the morphology of the fresh OCMs while the elemental composition was studied by EDX. The obtained particles had an irregular shape due to the kind of preparation methods used, including a pellet crushing step. The morphology of the surface of several OCM particles, LSF-30Fe-Pec-P, LSF-30Fe-MM-P, LSF-30Fe-Pec-20-40 and LSF-30Fe-Pec-MM-20-40, is shown in Fig. 2. The samples prepared by the Pechini method (a, c) were more porous than those obtained by mechanical mixing (b, d). Similar trends were obtained in the BET analyses with the samples prepared by the Pechini method having higher surface areas.

The elemental composition of the OCMs was studied by EDX analyses which proved that the desired composite structure, encapsulating iron oxide in an LSF731 matrix, was obtained using both preparation methods. Areas with a higher concentration of iron oxide were found in the particles when either sub-micron iron oxide powders or 20–40 μm iron oxide powders were used during the preparation. As an example, Fig. 3 shows a SEM and EDX of the LSF-30Fe-MM-20-40 OCM. Iron oxide is in the form of layers, typical of the structure of haematite, while LSF731 is in the form of small granules. Grain boundaries can be distinguished. Fig. 3b shows the EDX analysis of the same OCM which confirms the presence of iron oxide in specific areas of the particle surrounded by the LSF731.

Formation of the desired phases, iron oxide and LSF731, was confirmed by XRD analyses (not shown here) of the composite materials prepared by either mechanical mixing or a modified Pechini method. Reaction between iron and strontium to form strontium ferrites at high temperature could take place to a small extent during the preparation of the composite materials. Nevertheless, this interfacial phase was not detected in the XRD analyses performed. Galinsky et al. [9] found that strontium ferrite phase coexisted with the perovskite and iron oxide due to an incomplete solid-state reaction during the preparation of a composite material. After the first redox cycle in a TGA, the ferrite was incorporated to the LSF structure.

3.1.1. Effect of the cluster size

In order to determine if the size of the iron oxide clusters in the composite structure could have an effect on the reactivity of the OCMs, a preliminary study was carried out in the TGA. Iron oxide particles of different sizes (40–80 μm, 80–160 μm) and sub-micron powder were tested feeding carbon monoxide during the reduction and carbon dioxide during the oxidation at 850 °C and atmospheric pressure. Fig. 4 shows the normalised weight gain during the reduction and the oxidation, respectively, during the first and the third redox cycle. The weight variation was normalised by dividing by the expected available oxygen in the iron

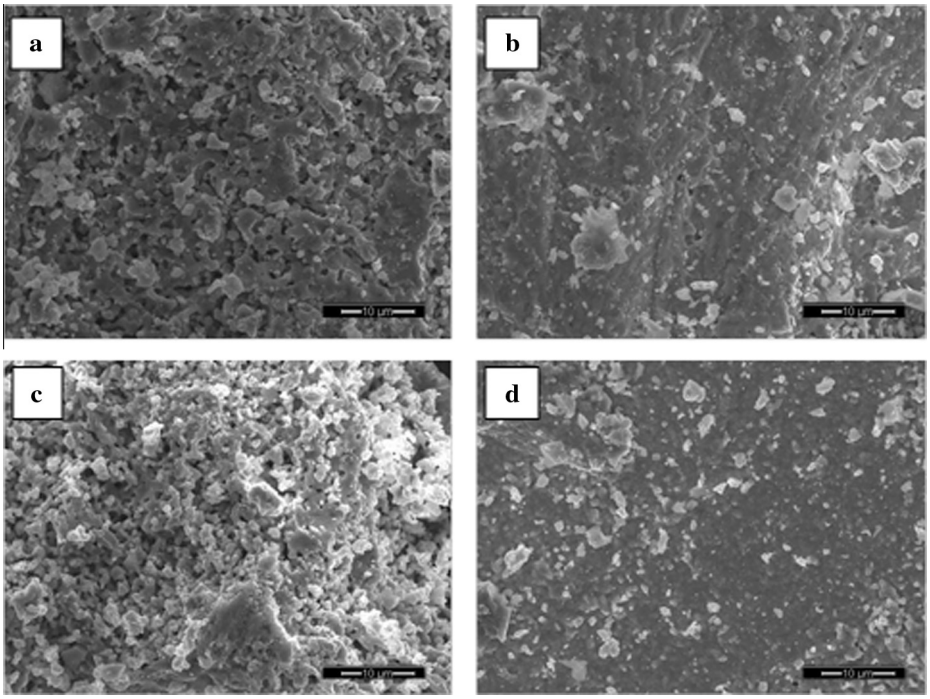

Fig. 2. SEM pictures of (a) LSF-30Fe-Pec-P, (b) LSF-30Fe-MM-P, (c) LSF-30Fe-Pec-20-40 and (d) LSF-30Fe-MM-20-40.

Please cite this article in press as: Dueso C et al. High-stability, high-capacity oxygen carriers: Iron oxide-perovskite composite materials for hydrogen production by chemical looping. Appl Energy (2015), http://dx.doi.org/10.1016/j.apenergy.2015.05.062

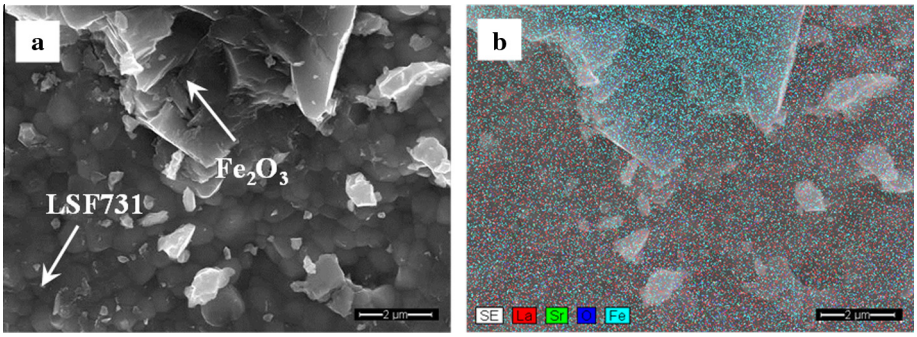

Fig. 3. (a) SEM picture and (b) EDX analysis of LSF-30Fe-MM-20-40.

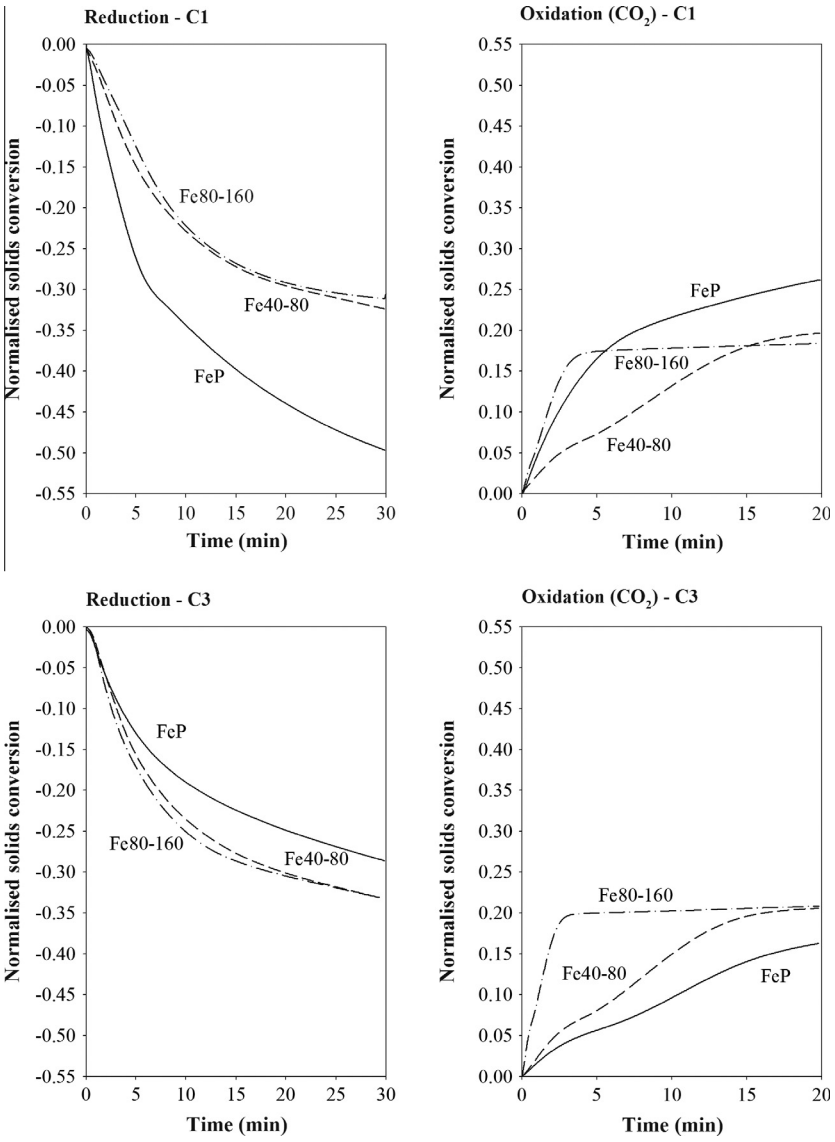

Fig. 4. Weight loss and weight gain during the reduction and the oxidation, respectively, of the first and third redox cycles for particles of iron oxide with different sizes (80–160 μm and 40–80 μm) and sub-micron powders. Reduction: 10% carbon monoxide in nitrogen; Oxidation: 10% carbon dioxide in nitrogen; Temperature: 850 °C.

oxide, assuming that it starts in the form of Fe_2O_3. During the reduction period of the first cycle, the sub-micron powder, FeP, was reduced faster and to a significantly higher extent than the iron oxide particles (Fe40-80 and Fe80-160). This could be related to the surface area of the particles shown in Table 1. FeP had a surface area two orders of magnitude higher than Fe80-160. Therefore the diffusional lengthscales required to access the oxygen are shorter. In the third cycle, a significant decrease in weight loss was observed for the iron powders, FeP, while the larger particles Fe40-80 and Fe80-160 showed little difference in

Please cite this article in press as: Dueso C et al. High-stability, high-capacity oxygen carriers: Iron oxide-perovskite composite materials for hydrogen production by chemical looping. Appl Energy (2015), http://dx.doi.org/10.1016/j.apenergy.2015.05.062

weight loss. It is believed that FeP experienced sintering and agglomeration increasing the particle size to lengthscales that are now in excess of the diffusional lengthscale. During the oxidation, a similar reduction in weight gain was observed for the iron oxide powders due to sintering or agglomeration. Values for the 80–160 μm and 40–80 μm particles were similar in both cycles, although the larger particles presented a higher oxidation rate. Thermal treatment of the particles during the preparation could cause sintering and grain growth. As grain boundary diffusion could be the rate determining step, during reaction the grain structure would be expected to influence kinetics, explaining the results shown in Fig. 4. It must be highlighted that FeP was not subjected to sintering at 1250 °C as were Fe40-80 and Fe80-160. Operation at high temperature favoured the sintering of the sub-micron iron oxide powders.

The oxygen consumed, summarised in Table 2, was calculated as the number of oxygen micromoles gained by the sample during the oxidation normalized with respect to the total amount of oxygen micromoles present in the iron oxide (as Fe_2O_3). Only between 16% and 26% of this oxygen was involved in the oxidation reaction suggesting that oxidation kinetics with CO_2 were slow.

Results obtained with the iron oxide particles of different sizes (sub-micron, FeP, 40–80 μm and 80–160 μm) in Table 2 and Fig. 4, illustrated that the highest reactivity corresponded to the commercial sub-micron powders during the first redox cycle. This suggests that if these iron oxide powders could be well dispersed into a LSF731 matrix, avoiding agglomeration and sintering, a significant increase in the reactivity of the composite material should be observed. To analyze the effect of the nominal cluster size on the reactivity several tests were performed in the TGA under the same operating conditions as experiments in Fig. 4. No clear effect of the cluster size was observed. SEM-EDX analyses of the composite OCMs demonstrated that the size of the iron oxide clusters was on the scale of 20 μm despite the initial cluster size used during the preparation (Fig. 3). Agglomeration of the sub-micron powders took place then during the OCM preparation. This could explain the similarities in the reactivity tests when sub-micron iron oxide and 20–40 μm powders were used.

Table 2
Oxygen consumption during the oxidation period of the first and the third redox cycle in the TGA for iron oxide particles with different particle size.

Iron oxide sample	Oxygen consumed (μmol O/μmol O in iron oxide)	
	Cycle 1	Cycle 3
FeP	0.26	0.16
Fe40-80	0.19	0.21
Fe80-160	0.18	0.21

3.2. Reactivity of the composite materials

The reactivity of the composite materials was studied in a TGA performing CO/CO_2 redox cycles at 850 °C. Fig. 5 shows the normalised solids conversion obtained during the third redox cycle. The normalised solids conversion was defined as the ratio between the weight gain during the reduction or oxidation with respect to the expected available oxygen.

$$\textit{Normalised solids conversion} = X = \frac{\Delta m}{\textit{Expected available oxygen}} = \frac{\Delta m}{(\alpha \cdot R_{O,Fe_2O_3} + (1-\alpha)\cdot R_{O,LSF731}\cdot\beta)\cdot m} \quad (4)$$

where Δm is the weight gain of the sample, m is the actual sample weight, α is the weight fraction of iron oxide in the OCM (30% or 11%) and $R_{O,Fe2O3}$ and $R_{O,LSF731}$ are the oxygen capacities of iron oxide and LSF731, respectively. The oxygen capacity of an OCM, R_O, can be calculated as:

$$R_O = \frac{m_{ox} - m_{red}}{m_{ox}} = \frac{3\cdot M_O}{M_i} \quad (5)$$

where m_{ox} is the weight of the fully oxidised form of the OCM and m_{red} is the weight of the fully reduced form. M_O is the molecular weight of oxygen and M_i is the molecular weight of either LSF731 or Fe_2O_3. For iron oxide, $R_{O,Fe2O3}$ would be 30% when Fe_2O_3 is reduced completely to Fe, and $R_{O,LSF731}$ is equal to 21.1%. As not all the oxygen in the LSF731 is available to react, an additional coefficient, β, is required. β is the weight fraction of available oxygen

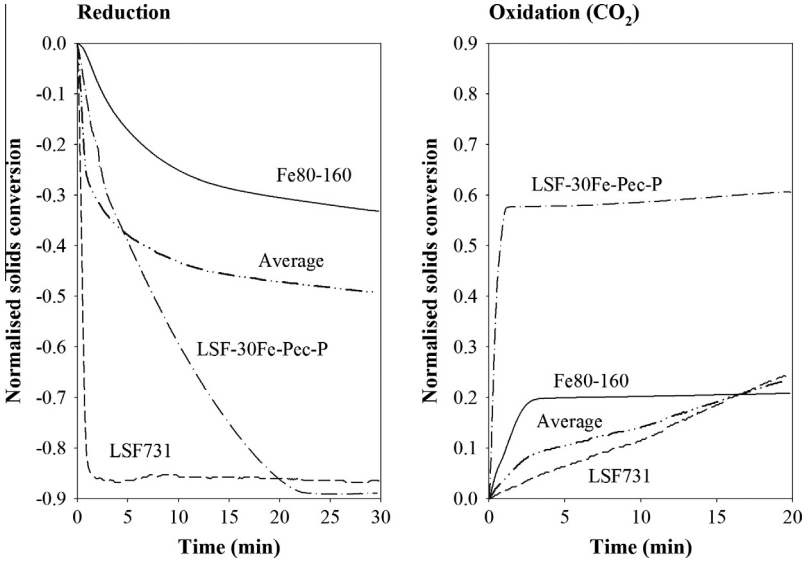

Fig. 5. Normalised solids conversion for the reduction and oxidation of (___) Fe80-160, (_ _ _) LSF731 and (_.._) LSF-30Fe-Pec-P during the third redox cycle in the TGA. (·····) Average normalised solids conversion considering the weight fraction of oxygen from LSF731 and iron oxide is included in the figure. Reduction: 10% carbon monoxide in nitrogen; Oxidation: 10% carbon dioxide in nitrogen; Temperature: 850 °C.

Please cite this article in press as: Dueso C et al. High-stability, high-capacity oxygen carriers: Iron oxide-perovskite composite materials for hydrogen production by chemical looping. Appl Energy (2015), http://dx.doi.org/10.1016/j.apenergy.2015.05.062

from the LSF731 which was obtained from the first redox cycle in the TGA, equal to 6.1 wt.%.

The normalised solids conversion and reaction rate for LSF731 appear high during reduction. The slope of the LSF731 can be deceptive, however, as significantly less oxygen is available due to the beta coefficient associated with the perovskite. The iron oxide, on the other hand, has very high oxygen availability yet the normalised solids conversion appears much lower. This is due the slow kinetics of iron oxide reduction.

The average normalised solids conversion at any time shown in Fig. 5, was modelled as the addition of the individual normalised solid conversion of LSF731 and iron oxide multiplied by the respective weight fraction of available oxygen in the OCM coming from the iron oxide, γ_{Fe2O3}, or the LSF731, γ_{LSF731}.

$$\gamma_{Fe_2O_3} = \frac{\alpha \cdot R_{O,Fe_2O_3}}{\alpha \cdot R_{O,Fe_2O_3} + (1-\alpha)\cdot\beta\cdot R_{O,LSF731}} \quad (6)$$

$$\gamma_{LSF731} = \frac{(1-\alpha)\cdot\beta\cdot R_{O,LSF731}}{\alpha \cdot R_{O,Fe_2O_3} + (1-\alpha)\cdot\beta\cdot R_{O,LSF731}} \quad (7)$$

$$Average_t = \gamma_{Fe_2O_3}\cdot X_{Fe_2O_3} + \gamma_{LSF731}\cdot X_{LSF731} = \gamma_{Fe_2O_3}\cdot\frac{\Delta m_{Fe_2O_3,t}}{R_{O,Fe_2O_3}\cdot m_{Fe_2O_3,0}} + \gamma_{LSF731}\cdot\frac{\Delta m_{LSF731,t}}{R_{O,LSF731}\cdot\beta\cdot m_{LSF731,0}} \quad (8)$$

where $m_{i,0}$ is the initial weight of the solid i, and $\Delta m_{i,t}$ is the weight gain at any given time, t. Sub-script i is either iron oxide or LSF731.

The absolute value of the LSF-30Fe-Pec-P normalised solids conversion was higher than the average during both the reduction and oxidation. This seems to indicate that the reactivity of this material did not correspond just to the simple additive model proposed (Eq. (8)). This improvement in reactivity could be due to the inhibition of sintering and agglomeration of the iron oxide when well dispersed within the LSF731 matrix. It would be possible to construct an average normalised solids conversion using the results from the first reduction (shown in Fig. 4) with sub-micron iron oxide powder; sintering being yet to occur to a high extent. Regardless of if the average is calculated from first or third cycle conversions, or if sub-micron powder, FeP, or particles, Fe80-160, of iron oxide are used, the composite material, LSF-30Fe-Pec-P, always performs better than any average model. This improvement must be due to a synergetic effect. It is suggested that the structure of the composite material enhanced the availability of oxygen and, therefore, the hydrogen production, as shown below.

The rate of oxygen uptake was calculated as the first derivate of the moles of oxygen reacted during the oxidation with time. The composite material LSF-30Fe-Pec-P showed an enhanced rate of oxygen uptake during the oxidation with carbon dioxide compared to iron oxide and LSF731 alone, as shown in Fig. 6.

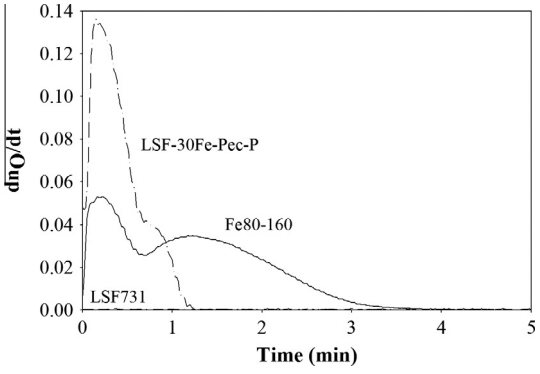

Fig. 6. Rate of oxygen uptake during the oxidation period of the third redox cycle working with (___) Fe80-160, (___) LSF731, and (_._._) LSF-30Fe-Pec-P as OCMs. Oxidising agent: 10% carbon dioxide in nitrogen; Temperature: 850 °C.

3.3. Cyclic operation in the microreactor

Several experiments were carried out in the CATLAB in order to determine the hydrogen produced with different LSF731- and iron oxide-containing OCMs and the stability of these materials over a larger number of cycles. The sample (50 mg) was initially pre-oxidised with 5% oxygen in helium. After that, 25 cycles using 5% carbon monoxide in helium during the reduction and 5% water in helium during the oxidation were performed at 850 °C and 1 atm.

Fig. 7 shows the gas molar fractions measured with the QMS during the 1st and 25th cycle for Fe80-160, LSF731, and LSF-30Fe-Pec-P OCMs. Sharp initial carbon monoxide peaks at the beginning of the reduction were due to valve changes and backpressure in the CATLAB system and should be ignored. A mixture of hydrogen and water was always obtained when the oxidation period started and pure hydrogen was not detected in any case.

In the case of Fe80-160, a decrease in the carbon dioxide and hydrogen production was observed during the reduction and the oxidation, respectively, with the number of cycles. Evidence for phase changes could not be distinguished in terms of any kinetic impact on the outlet gas phase mole fractions. When LSF731 was used, hydrogen was formed only for a very short period of time. A very narrow peak can be observed in Fig. 7. Nevertheless, the shape of the curves was the same during the 1st and the 25th cycle, indicating that the material behaviour was stable with time as demonstrated by Murugan et al. [8] in a previous work. Carbon dioxide and hydrogen production were much higher using the composite material LSF-30Fe-Pec-P than with either the LSF731 or iron oxide alone. A larger peak was obtained with clear kinetic evidence of what may be phase transitions between Fe–FeO and FeO–Fe_3O_4. Mass balances showed that, within measurement uncertainty, carbon formation did not take place with any of the OCMs.

The hydrogen production in micromoles, calculated from the integral of the hydrogen mole fraction versus time data, is depicted in Fig. 8. Although the Fe80-160 OCM was more stable than the iron oxide sub-micron powder, FeP, during the experiments performed in the TGA and was capable of maintaining reactivity over three cycles, a significant decrease in hydrogen production was observed over 25 cycles in the CATLAB. With LSF731 or LSF-30Fe-Pec-P, the hydrogen production remained constant after the few cycles that were needed for stabilization. The hydrogen production with LSF-30Fe-Pec-P in micromoles (367 μmol) during the oxidation period of the 25th cycle was 8 times higher than the production with Fe80-160 (46 μmol) and 4 times higher than the production obtained with the LSF731 (93 μmol). The expected available oxygen (Eq. (4)) for each material is equivalent to the expected amount of hydrogen production on a weight basis. In micromoles, the expected amount of hydrogen that could be obtained using the LSF-30Fe-Pec-P is 299 μmoles. LSF-30Fe-Pec-P produced 23% more hydrogen than expected. This indicates that the perovskite is more reducible in the composite form. This may be related to the synergetic behaviour observed in the TGA data.

3.3.1. Effect of the preparation method and the iron oxide content

Fig. 9 shows the hydrogen produced during the oxidation period with 5% water in helium using OCMs with 30 and 11 wt.% iron oxide fractions. The micromoles of hydrogen produced were lower when the material was prepared by mechanical mixing. It is suggested that the higher porosity of the OCMs prepared by Pechini method facilitated redox processes, improving the water splitting and increasing the amount of hydrogen produced. The micromoles of hydrogen obtained with the OCMs containing 11 wt.% of iron oxide were lower than with 30 wt.% of iron oxide as expected.

Please cite this article in press as: Dueso C et al. High-stability, high-capacity oxygen carriers: Iron oxide-perovskite composite materials for hydrogen production by chemical looping. Appl Energy (2015), http://dx.doi.org/10.1016/j.apenergy.2015.05.062

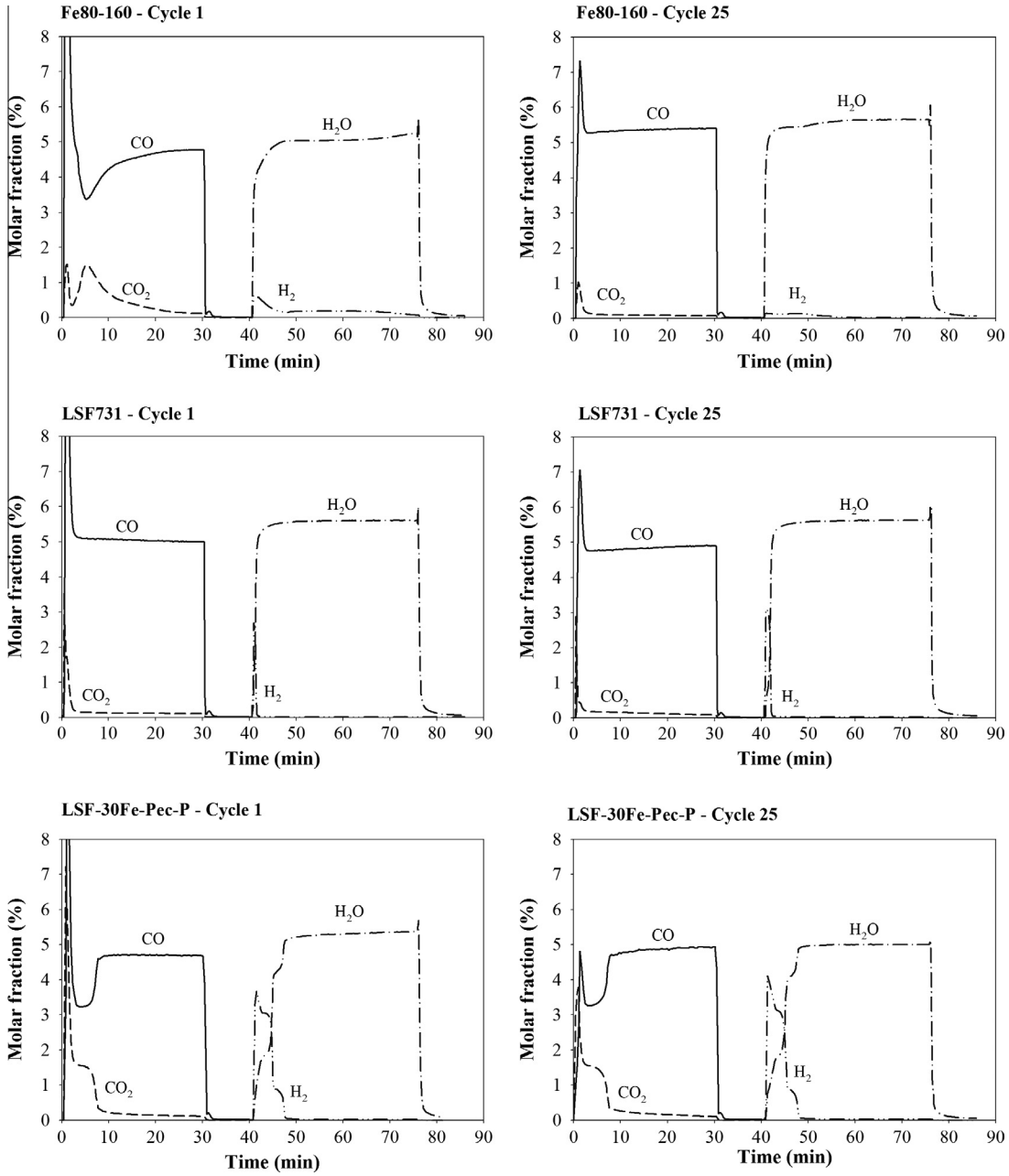

Fig. 7. Mole fraction during the 1st and 25th reduction and oxidation using Fe80-160, LSF731 and LSF-30Fe-Pec-P as OCMs. Reduction: 5% carbon monoxide in helium; Oxidation: 5% water in helium; Temperature: 850 ºC. Approximate sample mass: 50 mg.

The expected available oxygen of the OCMs is dominated by the iron oxide since the fraction of reducible oxygen in the LSF731 was very low. When the hydrogen production was normalized with respect to the expected available oxygen in the samples, there was no significant influence of the iron oxide content on the amount of hydrogen produced. As in the previous section, all the composite materials formed more hydrogen than expected considering that only 6.1 wt.% of the oxygen in the LSF731 was active for the process (β). The synergetic effect in the composite materials was observed again.

From an industrial point of view, a material with a higher content of iron oxide would be more suitable as it would allow a higher hydrogen production at a lower cost due to the lower LSF731 fraction. To prepare the large quantities of OCM needed in an industrial installation, a preparation method as simple as possible should be used. This would reduce the steps and time needed to get the final material and, as a consequence, the cost

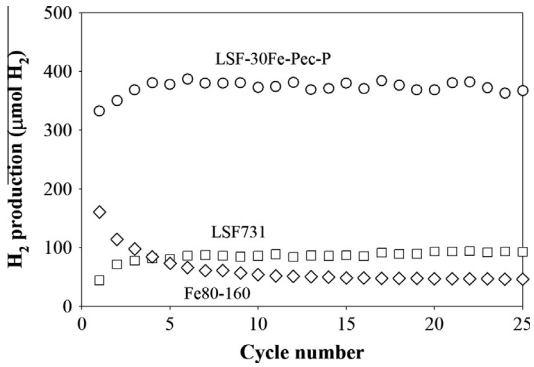

Fig. 8. Hydrogen production in µmol during isothermal cycling in the CATLAB with (◇) Fe80-160, (□) LSF731 and (○) LSF-30Fe-Pec-P as OCMs. Reduction: 5% carbon monoxide in helium; Oxidation: 5% water in helium; Temperature: 850 °C. Approximate sample mass: 50 mg.

Please cite this article in press as: Dueso C et al. High-stability, high-capacity oxygen carriers: Iron oxide-perovskite composite materials for hydrogen production by chemical looping. Appl Energy (2015), http://dx.doi.org/10.1016/j.apenergy.2015.05.062

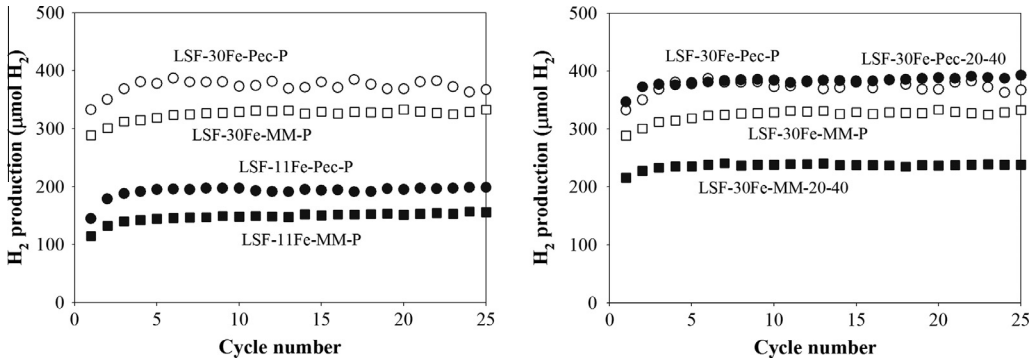

Fig. 9. Hydrogen production during isothermal cycling in the CATLAB (a) Effect of the preparation method and (b) effect of the cluster size. Reduction: 5% carbon monoxide in helium; Oxidation: 5% water in helium; Temperature: 850 °C. Approximate sample mass: 50 mg.

of the manufacture. Results obtained with the OCM prepared by Pechini method or MM were very similar in terms of hydrogen production. This suggests that the more involved Pechini method adds no extra value and the simple mechanical mixing method would be sufficient to prepare a composite OCM with better performance than the individual components.

Values of hydrogen production were similar using either Fe_2O_3 sub-micron powders during the preparation or 20–40 μm powders as can be seen in Fig. 9b. Differences observed between the OCMs LSF-30Fe-MM-P and LSF-30Fe-MM-20-40, both prepared by mechanical mixing, are due to a different mass of the sample used in the CATLAB. Data shown in the graph are not normalized.

4. Conclusions

In this work, the behaviour of several OCMs composed of LSF731 and iron oxide for hydrogen production by chemical looping was investigated. The objective was to obtain a composite structure with iron oxide clusters well dispersed and embedded in an LSF731 matrix. The OCMs were prepared by two different methods, i.e. mechanical mixing and a modified Pechini method, with different iron oxide weight fractions, 11 and 30 wt.%. SEM pictures and EDX analysis confirmed that the desired structure could be obtained. Although sub-micron powder and 20–40 μm powder of iron oxide were used to study the effect of the iron oxide nominal cluster size on reactivity, a clear conclusion could not be made since some agglomeration of the sub-micron powder took place during the preparation resulting in little difference between actual cluster sizes.

CO/CO_2 redox cycles performed in a TGA with LSF-30Fe-Pec-P showed that the reactivity of the composite OCMs did not merely correspond to the proportional addition of the oxygen capacities of both individual components, LSF731 and iron oxide. There was a synergetic effect resulting in a higher capacity of the composite material.

The stability of the composite materials for hydrogen production was studied in a microreactor, reducing with 5% carbon monoxide in helium and oxidising with 5% water in helium at 850 °C over 25 redox cycles. Hydrogen production was stable for LSF731 and LSF-30Fe-Pec-P but iron oxide particles (80–160 μm) experienced a decrease in hydrogen production due to agglomeration. The hydrogen production in micromoles during the oxidation of the 25th cycle was eight times higher for the composite material than for iron oxide and four times higher than for LSF731 alone. A 23% increase in the expected hydrogen production, equivalent to the expected available oxygen, was observed for LSF-30Fe-Pec-P. This suggests that LSF731 is more reducible when part of the composite material.

The results demonstrate that composite OCMs for chemical looping can be rationally designed. Dispersion of small iron oxide clusters within an LSF731 matrix avoids iron oxide agglomeration while the perovskite facilitates oxygen transport to and from the iron oxide. A combination of both compounds in the OCM particles allows an increase in the amount of hydrogen obtained in a chemical looping water–gas shift process.

Acknowledgements

Authors wish to thank Dr Stuart Scott, Wen Liu and Mohammad Ismail from Cambridge University for their help with the TGA work. CD thanks EPSRC for funding via a PLATFORM Grant, EP/G012865/1. CT thanks EPSRC for funding via a doctoral training award.

References

[1] Thursfield A, Murugan A, Franca R, Metcalfe IS. Chemical looping and oxygen permeable ceramic membranes for hydrogen production – a review. Energy Environ Sci 2012;5:7421–59.
[2] Hacker V, Fankhauser R, Faleschini G, Fuchs H, Friedrich K, Muhr M, et al. Hydrogen production by steam-iron process. J Power Sources 2000;86:531–5.
[3] Bohn CD, Müller CR, Cleeton JP, Hayhurst AN, Davidson JF, Scott SA, et al. Production of very pure hydrogen with simultaneous capture of carbon dioxide using the redox reactions of iron oxides in packed beds. Ind Eng Chem Res 2008;47:7623–30.
[4] Rydén M, Arjmand M. Continuous hydrogen production via the steam-iron reaction by chemical looping in a circulating fluidized-bed reactor. Int J Hydrogen Energy 2012;37:4843–54.
[5] Dennis JS, Scott SA. In situ gasification of a lignite coal and CO_2 separation using chemical looping with a Cu-based oxygen carrier. Fuel 2010;89:1623–40.
[6] Bohn CD, Cleeton JP, Müller CR, Chuang SY, Scott SA, Dennis JS. Stabilizing iron oxide used in cycles of reduction and oxidation for hydrogen production. Energy Fuel 2010;24:4025–33.
[7] Bouwmeester HJM, Kruidhof H, Burggraaf AJ. Importance of the surface exchange kinetics as rate limiting step in oxygen permeation through mixed-conducting oxides. Solid State Ionics 1994;72(2):185–94.
[8] Murugan A, Thursfield A, Metcalfe IS. A chemical looping process for hydrogen production using iron-containing perovskites. Energy Environ Sci 2011;4:4639–49.
[9] Galinsky NL, Huang Y, Shafiefarhood A, Li F. Iron oxide with facilitated O^{2-} transport for facile fuel oxidation and CO_2 capture in a chemical looping scheme. ACS Sustain Chem Eng 2013;1:364–73.
[10] Shafiefarhood A, Galinsky N, Huang Y, Chen Y, Li F. Fe_2O_3@$La_xSr_{1-x}FeO_3$ core-shell redox catalyst for methane partial oxidation. ChemCatChem 2014;6:790–9.
[11] Chen Y, Galinsky N, Wang Z, Li F. Investigation of perovskite supported composite oxides for chemical looping conversion of syngas. Fuel 2014;134:521–30.
[12] Galinsky NL, Shafiefarhood A, Chen Y, Neal L, Li F. Effect of support on redox stability of iron oxide for chemical looping conversion of methane. App Catal B-Environ 2015;164:371–9.
[13] Liu W, Dennis JS, Scott SA. The effect of addition of ZrO_2 to Fe_2O_3 for hydrogen production by chemical looping. Ind Eng ChemRes 2012;51:16597–609.

Please cite this article in press as: Dueso C et al. High-stability, high-capacity oxygen carriers: Iron oxide-perovskite composite materials for hydrogen production by chemical looping. Appl Energy (2015), http://dx.doi.org/10.1016/j.apenergy.2015.05.062